

INTERPRETING YOHKOH HARD AND SOFT X-RAY FLARE OBSERVATIONS

M. S. WHEATLAND and D. B. MELROSE

Research Centre for Theoretical Astrophysics School of Physics, University of Sydney, NSW 2006, Australia

(Received 29 August, 1994; in revised form 21 November, 1994)

Abstract. A simple model is presented to account for the *Yohkoh* flare observations of Feldman *et al.* (1994), and Masuda (1994). Electrons accelerated by the flare are assumed to encounter the dense, small regions observed by Feldman *et al.* at the tops of impulsively flaring coronal magnetic loops. The values of electron density and volume inferred by Feldman *et al.* imply that these dense regions present an intermediate thick-thin target to the energised electrons. Specifically, they present a thick (thin) target to electrons with energy much less (greater) than E_c where $15 \text{ keV} < E_c < 40 \text{ keV}$. The electrons are either stopped at the loop top or precipitate down the field lines of the loop to the footpoints. Collisional losses of the electrons at the loop top produce the heating observed by Feldman *et al.* and also some hard X-rays. It is argued that this is the mechanism for the loop-top hard X-ray sources observed in limb flares by Masuda. Adopting a simple model for the energy losses of electrons traversing the dense region and the ambient loop plasma, hard X-ray spectra are derived for the loop-top source, the footpoint sources and the region between the loop top and footpoints. These spectra are compared with the observations of Masuda. The model spectra are found to qualitatively agree with the data, and in particular account for the observed steepening of the loop-top and footpoint spectra between 14 and 53 keV and the relative brightnesses of the loop-top and footpoint sources.

1. Introduction

Recent observations by the *Yohkoh* spacecraft have provided new insight into the vexed question of the physical processes behind solar-flare hard and soft X-ray emission. For the first time the distribution of hard X-ray emission with height in the solar atmosphere has been unambiguously determined by well resolved observations of limb flares (Masuda, 1994). In this paper we are concerned with explaining some of the plasma physics of two specific sets of observations: those of Masuda and those of Feldman *et al.* (1994). By way of introduction, a summary is given of the main results of those observations.

Feldman *et al.* considered 38 impulsive X-ray flares observed with the high-resolution *Yohkoh* Soft X-ray Telescope (SXT). Typically, the emitting regions were found to be tiny pointlike sources (smaller than one SXT pixel, so $V \leq 3 \times 10^{18} \text{ m}^3$), surrounded by fainter extended emission. The diffuse emission defined a loop structure, with the pointlike emission at the top of the loop. The electron temperature for the point source was derived spectrally; for all flares observed, the peak temperatures were uniformly close to $2 \times 10^7 \text{ K}$. Feldman *et al.* argued that conduction cooling would be too slow to account for the observed decay in temperature of the bright features during the cooling phase. Also, the continued

Solar Physics **185**: 283–299, 1995.

© 1995 Kluwer Academic Publishers. Printed in Belgium.

appearance of the sources as pointlike during the cooling is inconsistent with conductive cooling along field lines. Assuming radiation cooling dominates, the cooling times observed imply a lower limit to the number density of electrons of order 10^{18} m^{-3} . An upper limit of $n_e = 10^{20} \text{ m}^{-3}$ was derived by Feldman *et al.* from line intensity ratios. Adopting the average emission measure $n_e^2 V = 3 \times 10^{54} \text{ m}^{-3}$ at peak intensity, these limits on density imply the corresponding range for the emitting volume $3 \times 10^{14} \text{ m}^{-3} < V < 3 \times 10^{18} \text{ m}^3$.

The values for electron number density derived by Feldman *et al.* are large compared with typical coronal ('quiet Sun') values, e.g., $n_e \approx 10^{14} \text{ m}^{-3}$ (Brown and McClymont, 1975). This observation provided the initial motivation for the model presented below.

The observations of Feldman *et al.* are at variance with the predictions of the 'chromospheric evaporation' model of the heating of the flare soft X-ray emitting plasma (Acton *et al.*, 1992). In the evaporation scenario, the hot, dense coronal flare plasma is supposed to be chromospheric material, evaporated from the footpoints of coronal loops by flare energy incident from above (Doschek *et al.*, 1990). The hot plasma should gradually rise up to fill the loop during the flare. These observations and others establish that the loop tops contain a region of dense, hot, soft X-ray emitting plasma early in the flare, implying that pre-existing, coronal plasma is heated *in situ* (Feldman, 1990). Any acceptable model of flare hard and soft X-ray emission must account for such *in situ* heating. Melrose and Dulk (1984), for example, developed a model for the *in situ* heating of the coronal soft X-ray emitting plasma through absorption of radio frequency emission produced by energetic electrons trapped in a flaring coronal loop.

Masuda (1994) presented simultaneous, coaligned hard and soft X-ray images, taken with the *Yohkoh* Hard X-ray Telescope (HXT) and the SXT, for two impulsive limb flares. These showed that, in addition to two footpoint hard X-ray sources, a hard X-ray source was located (in both cases) at or above the apex of the loop outlined in soft X-ray. A further analysis of ten limb flares observed with the HXT revealed three distinct types of hard X-ray sources associated with flares: footpoint sources (8 events/10), gradual loop-top sources (10/10) and impulsive loop-top sources (6/10). Masuda presented some estimates of the spectral indices of the footpoint and loop-top sources, based on the count ratios between adjacent energy bands of the HXT (see Section 4).

Masuda interpreted the presence of the loop-top hard X-ray source in the context of a theoretical model for flare energy release (e.g., Forbes and Malherbe, 1986). The mechanism of the energy release was considered to be magnetic reconnection, proceeding in a region some distance above the coronal loop of interest. The hypothesized reconnection outflow impinges on the loop, creating a shocked region just above the loop. The loop-top source observed by Masuda may be evidence for the presence of a shocked region, possibly where electrons are accelerated. In this paper we assume only that accelerated electrons are introduced by some

mechanism at the loop top, and account for the loop-top hard X-ray source observed by Masuda in terms of the interaction of the electrons with the ambient plasma.

The sections of this paper are divided as follows. In Section 2 a physical mechanism is outlined for the production of Masuda's loop-top and footpoint hard X-ray sources, as well as the loop-top soft X-ray sources described by Feldman *et al.* This is the basis in Section 3 for a detailed theoretical model of the photon spectra of the observed hard X-ray sources. In particular, the spectral indices of the model loop-top and footpoint sources are determined and an expression for their relative brightness derived. In Section 4 these model spectral indices and predictions about relative brightness are compared with Masuda's data. In Section 5 the energy going into heating the model loop-top source is written down and compared with the spectral observations of temperature obtained by Feldman *et al.* Section 6 contains a discussion of possible directions for improvement of the model, which is a prelude to future work. Finally, the main results of the model are summarised in Section 7.

2. Accounting for Footpoint and Loop-Top X-ray Sources

The bulk of the impulsive energy release in a solar flare goes into accelerating > 10 keV electrons. These electrons precipitate from near the apex of a coronal magnetic loop in both directions along field lines to the chromosphere. In the denser layers of the solar atmosphere the electrons encounter a thick target (Brown, 1971) and are stopped, producing the hard X-ray footpoint sources observed by Masuda (1994) and a wealth of secondary flare emission. We assume that the accelerated electrons are introduced by some means at the centre of the dense loop-top regions observed by Feldman *et al.* (1994) in soft X-rays. All the electrons then traverse, on average, half the dense region in escaping along field lines into the thinner, ambient coronal plasma.

In escaping the dense region at the top of the flaring coronal loop, the accelerated electrons traverse an intermediate thick-thin target. A given column depth of material is a thin target to a non-thermal distribution of electrons if that electron distribution remains unchanged in traversing the target. A thick target is a column depth of material sufficient to stop all the non-thermal electrons. The dense loop-top region considered here has a column depth such that it stops low-energy electrons in the injected electron flux spectrum, but does not stop high-energy electrons in the spectrum. This may be demonstrated as follows. The mean free path for an electron of energy E is $\lambda(E) = E^2 / (n_e K)$, with $K = 2\pi r_0^2 (m_e c^2)^2 \ln \Lambda$, where r_0 is the classical radius of the electron and $\ln \Lambda$ is the Coulomb logarithm. For a given column depth, $N_0 = n_e l$, the transition between thick and thin target occurs at an energy E_c defined by $l = \lambda(E_c)/2$, giving $E_c = (2KN_0)^{1/2}$. The values of Feldman *et al.* for n_e and V (quoted above) imply a range of column densities $10^{24} \text{ m}^{-2} < n_e V^{1/3} < 7 \times 10^{24} \text{ m}^{-2}$. The lower value of column density

corresponds to a larger, less dense source ($V = 3 \times 10^{18} \text{ m}^3$, $n_e = 10^{18} \text{ m}^{-3}$). Assuming that accelerated electrons are introduced at the centre of the dense region, and that they encounter half this column density on their outward path, implies $15 \text{ keV} < E_c < 40 \text{ keV}$. Here the values of $\ln \Lambda$ appropriate for a hydrogen plasma with $T_e = 10^7 \text{ K}$ and the number density quoted above are used in each case (Spitzer, 1962), namely $\ln \Lambda = 16$ ($n_e = 10^{20} \text{ m}^{-3}$) and $\ln \Lambda = 18$ ($n_e = 10^{18} \text{ m}^{-3}$). The range of non-thermal electron energies of relevance to solar flares is 10–100 keV. Consequently, a significant fraction of electrons in the accelerated electron population have energy $E < E_c$ and so are likely to be stopped at the top of the loop. This process may provide the heating of the loop-top source necessary to make it visible in soft X-ray (Feldman *et al.*) and also produces some hard X-rays. It is argued here that this is the mechanism responsible for the loop-top hard X-ray sources observed in limb flares by Masuda. The loop-top soft X-ray source is produced by the heating of pre-existing dense coronal material, and so avoids the weakness of the chromospheric evaporation model discussed above.

3. A Detailed Model for the Spectra of the Loop-Top and Footpoint Sources

A power-law electron flux spectrum $F_0(E) = AE^{-\delta}$ (electrons per unit time and per unit energy E) is assumed to be injected by the flare energy release mechanism in the centre of a dense cylindrical region of column depth $2N_0$ located at the apex of a coronal loop. This simple geometry implies that all electrons encounter the column depth N_0 in escaping into the ambient coronal loop plasma.

3.1. EVOLUTION OF THE ELECTRON FLUX SPECTRUM

To describe the X-ray spectrum of an intermediate thick-thin target accurately, it is necessary to describe how the electron distribution changes in traversing the target (Leach and Petrosian, 1981, 1983). This is in contrast to the thick or thin target limits, where only the injected electron flux spectrum needs to be specified (Brown, 1971). The treatment here follows Brown and McClymont (1975). For simplicity it is assumed that the electrons experience no change in average pitch angle as they traverse the dense region. Then the flux spectrum at column depth N has the analytic form

$$F(E, N) = \frac{EF_0(\sqrt{E^2 + 2KN})}{\sqrt{E^2 + 2KN}}, \quad (1)$$

cf., Brown and McClymont (1975) and Leach and Petrosian (1981). Note that it is assumed that the electron propagation time to the footpoints is much shorter than the time scale for variation of F_0 , so that the electron distribution in the flaring loop may be treated as static.

3.2. THE PHOTON SPECTRUM FROM THE LOOP-TOP

Following Brown and McClymont (1975), we adopt the non-relativistic, direction-integrated Bethe–Heitler cross-section for the production of bremsstrahlung photons in collisions of energized electrons with ambient particles. The spectrum (photons per unit time, per unit energy and per unit area at the Earth) of the loop-top source is then that of a source of column depth N_0 in which the electron flux spectrum is given by Equation (1). This may be written

$$I_{\text{lt}}(\epsilon) = I_{\text{th}}(\epsilon) - I'(\epsilon), \quad (2)$$

where $I_{\text{th}}(\epsilon)$ is the thick-target spectrum

$$I_{\text{th}}(\epsilon) = \frac{A\kappa_{\text{BH}}\bar{Z}^2}{4\pi R^2 K} \frac{B(\delta - 2, \frac{1}{2})}{(\delta - 2)(\delta - 1)} \epsilon^{-(\delta-1)}, \quad (3)$$

with $\kappa_{\text{BH}} = \frac{8}{3}\alpha r_0^2 m_e c^2$, and where α is the fine structure constant, $B(p, q)$ is the beta function, $R = 1$ AU and $\bar{Z} \approx 1.4$ is an average atomic number for the solar atmosphere. The second term on the right-hand side of Equation (2) represents the departure from thick-target behaviour and is given by

$$I'(\epsilon) = \frac{A\kappa_{\text{BH}}\bar{Z}^2}{4\pi R^2 K} \frac{\epsilon^{-(\delta-1)}}{\delta - 1} G(E_c/\epsilon, \delta), \quad (4)$$

with

$$G(\beta, \delta) = \int_0^1 x^{\delta-3} (1 + \beta^2 x^2)^{-(\delta-1)/2} f(x) dx, \quad (5)$$

and with $E_c = (2KN_0)^{1/2}$, $f(x) = \ln[(1 + \sqrt{1-x})/(1 - \sqrt{1-x})]$.

3.3. THE PHOTON SPECTRUM FROM THE FOOTPOINTS

Ignoring changes in $F(E, N)$ in propagating from the loop top to the footpoints, the footpoint source can be considered to be a thick target where the injection flux spectrum is $F(E, N_0)$, defined by Equation (1). This injection spectrum (illustrated in Figure 1) is depleted of low-energy electrons, which see the loop-top dense region as a thick target.

It then follows that the spectrum of the footpoint source is $I_{\text{fp}}(\epsilon) = I'(\epsilon)$, defined by Equation (4). This may be obtained by the usual thick target formulae with $F_0(E) = F(E, N_0)$ (e.g., Brown, 1975), or simply by recognising that, if unresolved, the sum of the loop-top and footpoint spectra must be the thick-target spectrum Equation (3). Hence Equation (2) must hold with $I'(\epsilon) = I_{\text{fp}}(\epsilon)$.

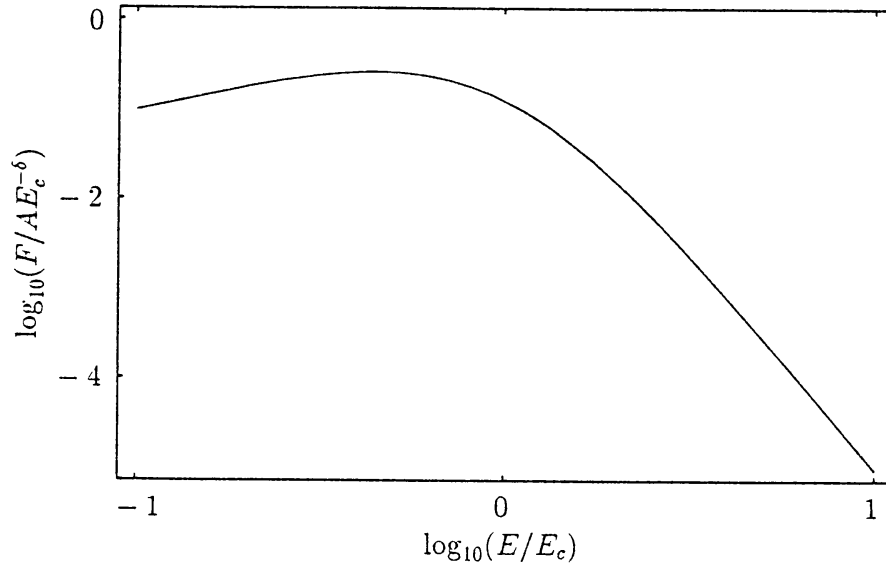


Fig. 1. The electron flux injection spectrum $F = F(E, N_0)$ for the footpoint source for the case $\delta = 5$. The spectrum is depleted below $E_c = (2KN_0)^{1/2}$. For $E \ll E_c$, $F \sim E$ and for $E \gg E_c$, $F \sim E^{-\delta}$.

3.4. THE PHOTON SPECTRUM FROM BETWEEN THE LOOP TOP AND FOOTPOINTS

If the electron flux spectrum is unchanged in propagating from the loop top to the footpoints, then the electrons must encounter a thin target between these two regions. A spectrum $I_a(\epsilon)$ may be calculated for bremsstrahlung from electrons stopped in the ambient coronal loop plasma by using the thin-target formulae (e.g., Brown, 1975) with the electron flux spectrum $F(E, N_0)$ and assigning a column depth N_a to the region. We find

$$I_a(\epsilon) = \frac{A\kappa_{\text{BH}}\bar{Z}^2}{4\pi R^2} N_a \epsilon^{-(\delta+1)} G'(E_c/\epsilon, \delta), \quad (6)$$

with

$$G'(\beta, \delta) = \int_0^1 x^{\delta-1} (1 + \beta^2 x^2)^{-(\delta+1)/2} f(x) dx. \quad (7)$$

3.5. BEHAVIOUR OF MODEL SPECTRA

Figure 2 shows the qualitative behaviour of the spectra I_{lt} and I_{fp} . The most important prediction of this model is clear from the figure, namely that both spectra show a break in (photon) spectral index γ about $\epsilon = E_c = (2KN_0)^{1/2}$, but the sum of the two spectra does not show a break in spectral index. $I_{\text{lt}} + I_{\text{fp}}$ is the spectrum of a thick target and so consists of a single power law (with index $\delta - 1$).

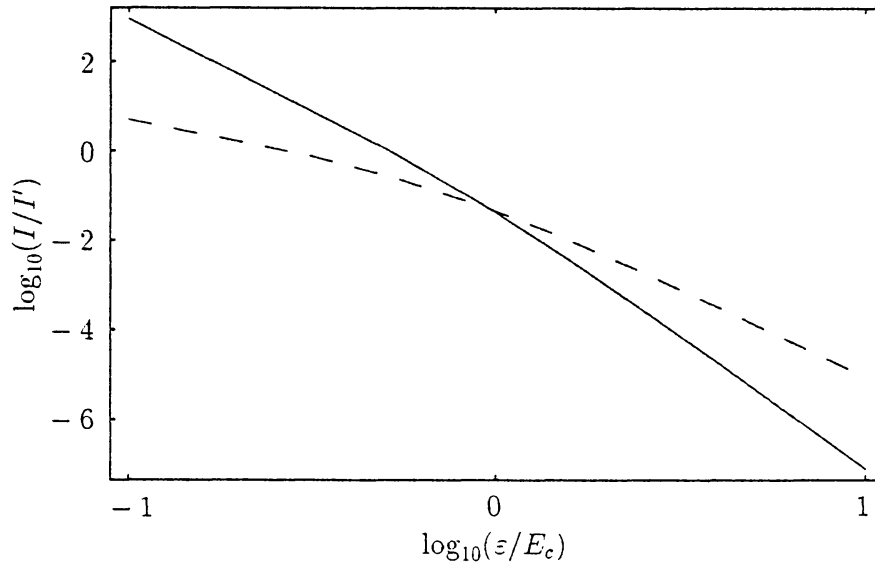


Fig. 2. The scaled photon spectra I_{lt}/I' (solid) and I_{fp}/I' (dashed) plotted as a function of ϵ/E_c , where $I' = 4\pi R^2 K / (A\kappa_{BH}\bar{Z}^2)$. The loop-top source approaches spectral indices $\delta - 1$ and $\delta + 1$ for $\epsilon \ll E_c$ and $\epsilon \gg E_c$, respectively. The footpoint source is not a power law for $\epsilon \ll E_c$ but is for $\epsilon \gg E_c$, when it approaches the thick-target index $\delta - 1$.

Equation (6) implies that the spectrum of the portion of the flux tube between the loop top and footpoints also exhibits a break in spectral index about $\epsilon = E_c$.

The breaks in index of the model spectra may be understood as follows. Consider first the behaviour of the spectra I_{lt} , I_{fp} , and I_a at high energies, i.e., when $\epsilon \gg E_c$. At high energies the loop-top source has the spectral index $\delta + 1$ – the spectral index of a thin target (Brown, 1975) – because high-energy electrons (responsible for the high-energy photons) see the loop-top region as a thin target. The footpoint source at high energies approaches a power law with index $\delta - 1$, because the injected spectrum at high energies is undepleted and these electrons meet a thick target at the footpoint. Finally, for high energies I_a becomes a power law with index $\delta + 1$, because it is a thin target to an undepleted electron spectrum. Next consider the behaviour of the model spectra at low energies, i.e., when $\epsilon \ll E_c$. At low energies, the spectral index of the loop top is $\delta - 1$, because low-energy electrons (which produce most of the low-energy photons) see the loop-top region as a thick target. The spectra I_{fp} and I_a are not power laws at low energy, because they are produced by a depleted electron flux spectrum.

The other important property of the spectra I_{lt} and I_{fp} , as seen in Figure 2 is that I_{lt} dominates over I_{fp} for $\epsilon \ll E_c$, whilst I_{fp} dominates for $\epsilon \gg E_c$. At $\epsilon = E_c$ they are equal in magnitude. This may be understood as follows. Low-energy photons are most likely to be produced by the stopping of low-energy electrons, which see the loop-top region as a thick target. Consequently the loop top is brightest at low photon energies. High-energy photons must be produced by high-energy electrons, which see the loop top as a thin target and so are likely to reach the footpoints.

Consequently the footpoints dominate the photon spectrum at high energies. The equivalence of the magnitude of the two spectra at $\epsilon = E_c$ provides an observational determination of E_c according to the model.

3.6. RATIO OF COUNT RATES

To compare the predictions of the model spectra with Masuda's data, a relevant quantity is the ratio of count rates between the footpoint source and the loop-top source above a cut-off energy ϵ_0 :

$$r(\epsilon > \epsilon_0) = \int_{\epsilon_0}^{\infty} I_{\text{fp}}(\epsilon) d\epsilon / \int_{\epsilon_0}^{\infty} I_{\text{lt}}(\epsilon) d\epsilon . \quad (8)$$

We find

$$r(\epsilon > \epsilon_0) = \left[\frac{B(\delta - 2, \frac{1}{2})}{(\delta - 2)\Gamma(\delta/2)J(\epsilon_0/E_c, \delta)} - 1 \right]^{-1} , \quad (9)$$

with

$$J(u, \delta) = (2u)^{(\delta-2)/2} \int_0^1 x^{(\delta-4)/2} [1 + (w/u)^2]^{(\delta-2)/4} \times \\ \times P_{(\delta-4)/2}^{(\delta-2)/2} \{ [1 + (x/u)^2]^{-1/2} \} f(x) dx , \quad (10)$$

where $P_{\nu}^{\mu}(x)$ is the associated Legendre function of the first kind (Abramowitz and Stegun, 1965). Plots are shown in Figure 3 of $r(\epsilon > \epsilon_0)$ as a function of ϵ_0/E_c over an appropriate range. The function $r(\epsilon > \epsilon_0)$ is a monotonically increasing function of ϵ_0/E_c . This is because the footpoint source is brighter at higher energies. Also, $r(\epsilon > \epsilon_0)$ decreases with δ . This is because steeper injection spectra imply more lower-energy electrons, which are likely to be stopped at the loop top, hence increasing the relative brightness of the loop-top source.

4. Comparison with Masuda's Observations

4.1. MASUDA'S SPECTRAL INDICES

Masuda's (1994) individual spectral indices for loop-top and footpoint sources for ten limb flares are reproduced in Table I. The quoted values are approximate, derived from count rates in adjacent energy bands under the assumption that a single power law holds over both bands. Specifically, spectral indices γ were inferred from the ratio of count rates of the L (14–23 keV) and M1 (23–33 keV) bands

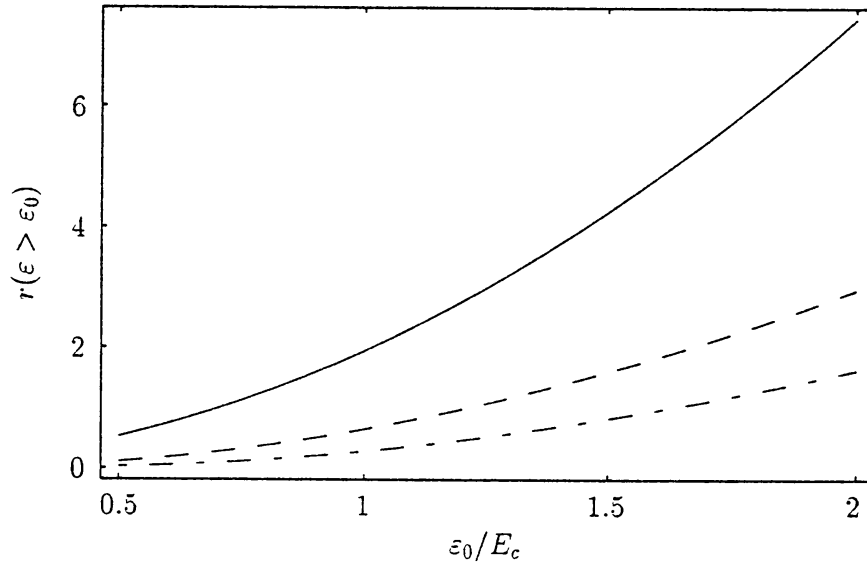


Fig. 3. The ratio $r(\epsilon > \epsilon_0)$ of counts per second at the footpoints to the loop top above a cut-off energy ϵ_0 plotted as a function of ϵ_0/E_c . The solid curve is for the case $\delta = 5$, the dashed curve is $\delta = 7$ and the dot-dashed curve is $\delta = 9$.

TABLE I

The spectral indices $\gamma(\text{M1/L})$ and $\gamma(\text{M2/M1})$ (see text) derived by Masuda (1994) for the footpoint (fp) and loop-top (lt) sources in the ten limb flares observed. Dashes indicate that one of the sources was not observed for that flare.

Date	$\gamma_{\text{lt}}(\text{M1/L})$	$\gamma_{\text{lt}}(\text{M2/M1})$	$\gamma_{\text{fp}}(\text{M1/L})$	$\gamma_{\text{fp}}(\text{M2/M1})$
2 Dec., 1991	5.5	5.5	3.2	6.3
15 Dec., 1991	—	—	3.5	3.9
13 Jan., 1992	2.6	4.1	≤ 2.0	4.0
6 Feb., 1992	6.8	≥ 9.0	—	—
17 Feb., 1992	5.4	≥ 9.0	2.7	6.7
1 Apr., 1992	—	—	3.2	3.7
4 Oct., 1991	≥ 2.0	5.2	2.3	3.4
5 Nov., 1992	—	—	3.9	6.5
23 Nov., 1992	5.5	6.3	3.8	4.6
17 Feb., 1993	3.6	6.1	4.1	6.0

(here denoted $\gamma(\text{M1/L})$) and the M1 and M2 (33–53 keV) bands ($\gamma(\text{M2/M1})$). No detailed spectra are possible with the *Yohkoh* instruments. Spectral indices derived from count rates in such broad adjacent energy bands are subject to considerable uncertainty. Consequently, care must be taken in the comparison of the spectral predictions of the model presented above and Masuda's data. Despite these caveats, our simple model qualitatively agrees with many aspects of Masuda's data.

Masuda observed localized footpoint and loop-top sources in the higher energy bands (M1, M2) and a more diffuse X-ray emission, following the soft X-ray loop, at lower energy (L). This qualitatively agrees with our model. The thin-target emission described by I_a is seen only at lower energies because higher-energy electrons (responsible for high-energy photons) are less likely to be stopped between loop top and footpoints. Masuda's loop-top and footpoint spectral indices are based on a procedure of drawing a box around each source and counting photons within the box for each energy band. This approach neglects the diffuse emission from the loop at lower energies. Consequently it is not possible to compare in detail the spectrum I_a predicted by Equation (6) and observation. In the remainder of this section we compare the model spectra I_{lt} and I_{fp} with Masuda's observations.

4.2. THE BREAK IN SPECTRAL INDEX

One striking aspect of Masuda's data is the break in spectral index, i.e., the difference between $\gamma(M1/L)$ and $\gamma(M2/M1)$. Steepening of (unresolved) flare impulsive hard X-ray spectra at high energies is a familiar observational fact (Brown, 1971) but occurs generally in the 60–100 keV range (and sometimes as high as 500 keV), significantly higher than the steepening inferred by Masuda for the individual, resolved loop-top and footpoint spectra. The change in γ in the unresolved case is generally less than two and is attributed to a fundamental change in the injected electron distribution at these energies. These comments refer to the early impulsive phase of hard X-ray emission. More detailed spectral behaviour is observed in the later stages of the flare (e.g., Lin *et al.*, 1981).

The model presented here predicts a break in spectral index for both the loop-top and footpoint sources at $\epsilon = E_c = (2KN_0)^{1/2}$, owing to the passage of the injected electrons through the intermediate thick-thin target at the loop apex. As explained in Section 2, the observations of Feldman *et al.* (1994) imply that E_c is in the range 15–40 keV. So the model accounts for the observed spectral break at the right energy.

The model also predicts that if the loop-top and footpoint sources are unresolved (so that only the sum of their spectra is relevant) no break in spectral index should be observed at E_c . It is not possible to test this prediction from Masuda's published data without a detailed knowledge of the instrumental response of the *Yohkoh* HXT (Takakura *et al.*, 1993). With the appropriate knowledge, this test of the model could be straightforwardly conducted.

The model presented above also predicts specific relations between the spectral indices of the loop top and footpoints at high and low energies. For example, the spectrum of the loop top at low energies (i.e., $\epsilon \ll E_c$) should be the same as that of the footpoint sources at high energies ($\epsilon \gg E_c$), namely $\delta - 1$. Masuda's data (in the cases where both footpoint and loop-top indices were available for the same event) roughly agree with this prediction. The greatest deviation is in the 17 February, 1993 event, where the indices of interest differ by 2.4. There is also

some evidence in Masuda's data for the other specific predictions, although there are individual discrepancies. The model also predicts that the footpoints have a harder spectrum than the loop-top source. Indirect evidence for this prediction is provided by the observation that the average height above the photosphere of hard X-ray sources observed by *Yohkoh* (based on about a hundred flares) decreases with increasing energy (Kosugi, 1993).

4.3. TYPE A FLARE OBSERVATION

Another piece of evidence for the model is provided by the event of 2 June, 1992, which was remarkable in two ways. The first is that, in the main (gradual) phase of the flare, only a loop-top source was observed, with no corresponding footpoint emission. The second is that the spectral indices derived were the largest of the set of observations. Masuda described this event as an example of a 'super-hot' or Type A flare. This event qualitatively agrees with the model presented above, as follows. As explained in Section 3, the relative brightness of the footpoint source is expected to decrease with increasing δ , as the bulk of the accelerated electrons have low energy and are stopped at the loop top (see Figure 3). For a steep enough injection spectrum and sufficient column depth N_0 , the footpoint source should not be visible at all. Interestingly, footpoint emission was observed by Masuda in an earlier, extremely hard impulsive episode from the same flare (Masuda's Figure 3.2). This also agrees with the model presented above: the earlier burst consisted of higher energy electrons (it was most prominent in the M2 and H bands) which escaped from the loop-top source to produce footpoint emission.

4.4. THE RELATIVE BRIGHTNESS OF THE FOOTPOINTS AND LOOP TOP

The expression (9) (and Figure 3) may be compared more generally with the observation by Masuda that the loop-top impulsive source is less intense than the footpoint sources by a factor ≤ 5 at energies ≥ 25 keV. As shown in Section 2, the observations of Feldman *et al.* imply that $15 \text{ keV} < E_c < 40 \text{ keV}$, so taking the cut-off energy $\epsilon_0 = 25 \text{ keV}$, $0.6 < \epsilon_0/E_c < 1.7$. Consulting Figure 3, for reasonable δ this range of ϵ_0/E_c does indeed imply a loop-top source less intense than the footpoint source by a factor less than about six. This result is subject to the caveat that Equation (9) does not include the instrumental response of the *Yohkoh* HXT (Takakura *et al.*, 1993).

5. The Heating of the Loop-Top Source

When electrons are stopped at the loop-top dense region, only a small fraction of the electron energy (typically $\approx 10^{-5}$) goes into producing hard X-rays. The bulk of the energy goes into collisional heating of the ambient plasma. Based on this fact, a simple model may be constructed of the heating of the loop-top source.

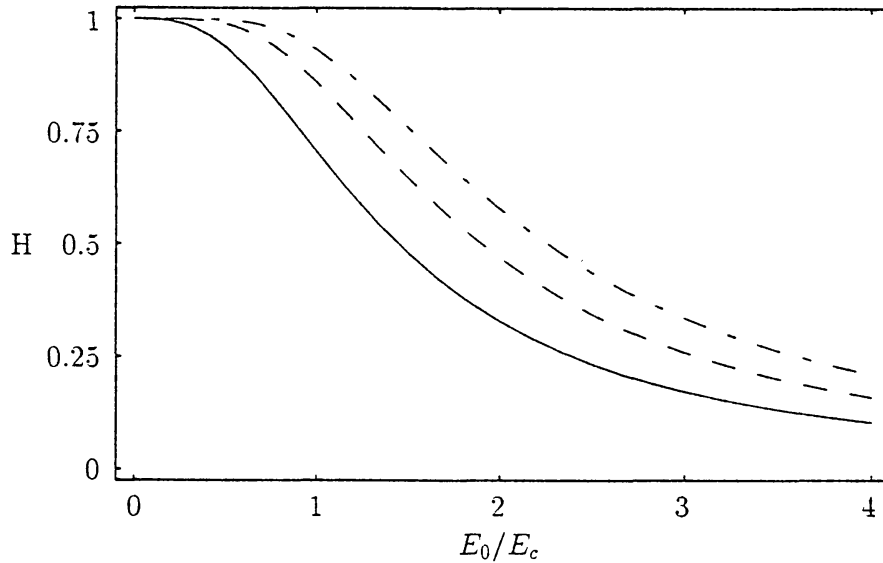


Fig. 4. The fraction of electrons stopped at the loop top, H , plotted as a function of E_0/E_c . The solid curve is for $\delta = 5$, the dashed curve $\delta = 7$, and the dot-dashed curve $\delta = 9$.

5.1. THE ENERGY DEPOSITED BY ELECTRON COLLISIONS AT THE LOOP TOP

The number of electrons stopped per second, per unit electron energy, E , in the dense region from $N = 0$ to $N = N_0$ is $\mathcal{N} = F_0(E) - F(E, N_0)$, and so the power deposited is $P = \int_{E_0}^{\infty} \mathcal{N} E dE$, where E_0 is the necessary cut-off at low energy in the injected electron spectrum. The quantity E_0 is probably around 10 keV, although it is difficult to determine observationally, and may be as high as 25 keV (Dennis, 1988). The expression for P may be evaluated to give

$$P = \frac{A}{\delta - 2} E_0^{-(\delta-2)} H(E_0/E_c, \delta), \quad (11)$$

with

$$H(\xi, \delta) = 1 - F[(\delta + 1)/2, (\delta - 2)/2; \delta/2; -\xi^{-2}], \quad (12)$$

where $F(a, b; c; x)$ is Gauss' Hypergeometric function (Abramowitz and Stegun, 1965). Equation (11) may be identified as containing the power injected if all the electrons are stopped, viz., $A E_0^{-(\delta-2)} / (\delta - 2)$, multiplied by a factor describing the fraction of electrons that are stopped (H). Figure 4 shows a plot of this fraction, for relevant δ as a function of E_0/E_c . Similar comments about the general behaviour of this function can be made to those following Equations (9) and (10) above.

Equation (11) gives P in terms of A , which is still undetermined. Masuda quoted the loop-top count rate in the M2 band (33–53 keV) for the 13 January flare during its impulsive phase at $0.22 \text{ cts s}^{-1} \text{ SC}^{-1}$, where SC refers to one of the 64 HXT subcollimators. The effective area of the HXT is 60 cm^2 , so

this corresponds to a photon count rate of $2350 \text{ cts s}^{-2} \text{ m}^{-2}$. If this count rate corresponds to $\int_{M2} I_{\text{lt}} d\epsilon$, where I_{lt} is given by Equation (2), then we can estimate A and hence P by Equation (11). This approach does not take into account the detailed instrumental response of *Yohkoh* (Takakura *et al.*, 1993), but is the best estimate possible with the available data. Taking $E_0 = 10 \text{ keV}$ and $\delta = 5$ we find $2 \times 10^{20} \text{ W} < P < 7 \times 10^{20} \text{ W}$, where the upper part of the range corresponds to the larger, less dense loop-top source ($n_e = 10^{18} \text{ m}^{-3}$, $V = 3 \times 10^{18} \text{ m}^3$). A characteristic impulsive time scale for the flares is about a minute, implying a total energy deposition at the loop-top in the range $1 \times 10^{22} - 4 \times 10^{22} \text{ J}$. This estimate is sensitively dependent on the cut-off energy E_0 . For example, taking $E_0 = 25 \text{ keV}$ instead of $E_0 = 10 \text{ keV}$, the inferred total deposited energy is in the range $6 \times 10^{20} - 1 \times 10^{21} \text{ J}$.

5.2. COMPARISON WITH THE OBSERVED HEATING OF THE LOOP TOP

Now let us compare the energy deposited by the energetic electrons with the energy required to account for the heating observed by Feldman *et al.* (1994). For all the 38 flares investigated by Feldman *et al.*, the maximum electron temperature observed was close to $T_e = 2 \times 10^7 \text{ K}$. This implies an energy input into the loop top source of order $n_e V k_B T_e$ and using the range of n_e and V derived by Feldman *et al.* we obtain the estimate of the energy going into heating the loop-top source $10^{19} - 10^{21} \text{ J}$, where the upper estimate corresponds to a larger, less dense loop-top region. Comparing this estimate with the previous calculation of the energy deposited at the loop top by the braking of electrons, clearly the $E_0 = 25 \text{ keV}$ estimate of the energy deposited may be consistent with the observed heating, but the $E_0 = 10 \text{ keV}$ estimate implies that significantly more energy is being deposited at the loop top by stopping electrons than appears in the heating of the loop top as observed by Feldman *et al.* This critical dependence on E_0 is a familiar problem in the context of flare electron beam energetics (Dennis, 1988). Certainly the model provides deposition of enough energy at the loop top by the process of stopping electrons to account for the heating observed by Feldman *et al.*

Another way of resolving the possible inconsistency between the model estimate of the energy deposited by electrons and the energy associated with the observed heating is in terms of an inhomogeneous model. Specifically, suppose that the loop-top region consists of regions of dense material embedded in less dense plasma. The denser material is heated less rapidly as the energetic electrons are stopped and because of the sensitive dependence of the response of the SXT to temperature (Tsuneta *et al.*, 1991) only the thinner material may be visible in soft X-ray. Then the dense regions produce hard X-rays when they stop electrons but no appreciable soft X-ray emission. The details of such a model for the heating of the loop-top region are being investigated.

6. Discussion

The model developed above accounts well for some of the wealth of observational detail provided by *Yohkoh*. Nevertheless, many questions remain to be answered. The most unsatisfactory aspect of the model is the description of the dense loop-top region and the introduction of the energetic electrons into this region. This part of the model is consistent with the few observational details provided by Feldman *et al.* (1994). However, the model does not address the deeper questions of the mechanisms of electron acceleration and more generally, of flare energy release. Dense coronal plasma is assumed to be located in a small region at the loop top at the onset of the flare. This region is presumably produced by the flare energy release mechanism. The electrons may be accelerated in the dense region itself, or perhaps they are accelerated at a remote site (above the loop) and precipitate to the loop-top region. The dense loop-top region is rapidly heated by impinging electrons, and so should expand along field lines. Feldman *et al.* reported that the impulsive soft X-ray sources observed remained pointlike throughout the period of observation, and so a mechanism for confinement of the heated plasma is implied. A more detailed and complete model must describe the physics of such a confinement process. The question is not addressed here, but will be the subject of future work.

Masuda's co-aligned soft and hard X-ray images appear to show a systematic displacement of 3/10 of the observed loop-top hard X-ray sources above the loop as outlined in soft X-ray. The best example is provided by the 13 January event (Masuda *et al.*, 1994). The apparent displacement of the hard X-ray source in these instances was interpreted by Masuda (1994) to indicate flare energy release occurring from above. The model presented above predicts spatially coincident loop-top soft and hard X-ray sources, since they arise from the interaction of energised electrons with the same dense region. Future observations will confirm or deny the reality of the displacement.

One flare-energy-release mechanism (involving the production of a dense loop-top region) is the theoretical model of Forbes and Malherbe (1986). Reconnection is assumed to proceed between magnetic field lines above the loop and a wedge-shaped shock is produced where one reconnection jet (outflow) impinges on the loop, near its apex. This model has not been sufficiently developed to predict the details of expected hard and soft X-ray emission at the loop top. The model developed above is compatible with Forbes and Malherbe's (1986) model because it allows the possibility that electrons are energised at a remote site, say above the loop, and then propagate along field lines to the dense loop-top regions.

As discussed above, the model may imply that more energy is deposited at the loop top than appears in soft X-ray, suggesting that this region may be highly non-uniform.

The model presented here has many restrictive assumptions that should be relaxed in a more realistic treatment. First, the change in the electron flux spectrum described by Equation (1) neglects changes in average pitch angle of the inject-

ed electrons. A more detailed description must take some account of this process (e.g., Leach and Petrosian, 1981). Magnetic mirroring of energetic electrons as they approach the stronger fields of the footpoints has also been neglected, although this may be an important aspect of the physics of electron precipitation to the chromosphere (e.g., Melrose and White, 1981). The gradually increasing density of the solar atmosphere with decreasing depth is treated here as step in density, identified with the chromospheric boundary. A more detailed model should incorporate a better description of the solar atmosphere.

7. Conclusions

A simple model is presented here to account for the *Yohkoh* soft and hard X-ray observations of Feldman *et al.* (1994) and Masuda (1994). The basis of the model is the assumption that 10–100 keV electrons accelerated by the flare traverse the dense, small regions observed in soft X-ray by Feldman *et al.* at the apex of flaring coronal loops. The values of density and volume derived by Feldman *et al.* imply that these regions present an intermediate thick-thin target to electrons passing outwards through them. Specifically, the regions represent a column depth $10^{24} \text{ m}^{-2} < N_0 < 7 \times 10^{24} \text{ m}^{-2}$ and are thick (thin) targets to electrons with energy much less (greater) than $E_c = (KN_0)^{1/2}$, with $15 \text{ keV} < E_c < 40 \text{ keV}$. A fraction of the accelerated electrons are stopped in the dense loop-top region, leading to heating of the loop-top region and production of hard X-rays via bremsstrahlung. The loop-top soft X-ray source is identified as a region of dense coronal material, which is present at the flare onset and which is heated *in situ* by energetic electrons impinging on it. This is in contrast to ‘chromospheric evaporation’ models in which the coronal soft X-ray emission is attributed to chromospheric material evaporated into the coronal loop from its footpoints. Coincident soft and hard X-ray flare observations favour *in situ* heating over evaporation (Feldman, 1990).

Adopting a simple model for the way in which electrons lose energy in precipitating to the footpoints, theoretical individual hard X-ray spectra are derived for the loop-top dense region, the thick-target sources at the footpoints of the loop, and the thin-target region between loop top and footpoints. The model loop-top and footpoint spectra are compared with the spectral estimates of Masuda, and the simple model is found to qualitatively agree with the data, although there are individual discrepancies. In particular, the model accounts naturally for the observed steepening in the spectral indices of both loop-top and footpoint sources between 14 keV and 53 keV, and predicts that there will be no corresponding steepening in the spectral index of the sum of the loop-top and footpoint sources. The model also provides an explanation for Masuda’s Type A or ‘super-hot’ flare observation of 6 February, 1992, when a loop-top hard X-ray source was seen with no corresponding footpoint emission. If the injected electron spectrum at the loop top is steep enough, and/or the column depth of the loop-top region is large enough, almost all the electrons are

stopped at the loop top, leading to only a loop-top source. More generally, the model spectra plausibly account for the observed relative brightnesses of the footpoint and loop-top sources. They also suggest an independent observational method of determining E_c , as the photon energy at which the loop-top and footpoint sources are equally bright.

The model allows the calculation of the energy deposited in the dense loop-top region by the braking of electrons. This is compared with the heating observed by Feldman *et al.* and the model implies that (at least) enough energy is deposited at the loop top to account for the heating observed in soft X-ray. Depending on the (observationally poorly constrained) choice of the low energy cut-off to the electron spectrum, it is possible that significantly more energy is deposited at the loop top than appears in soft X-ray. This discrepancy, if real, may suggest that the loop-top region is highly inhomogeneous. If the loop-top region consists of dense material embedded in less dense material, the energy deposited in the dense material may raise its temperature less than if the same energy were deposited in the less dense material. Hence the energy deposited in the dense material does not appear in soft X-ray.

In conclusion, our model qualitatively accounts for some details of recent *Yohkoh* hard and soft X-ray flare observations. The model is, however, clearly oversimplified and in particular does not address the central question of the mechanism of solar flare energy release. Further work, directed towards accounting for the details of the loop-top X-ray sources observed by Masuda may shed some light on this deeper problem.

References

- Abramowitz, M. and Stegun, I. A.: 1965, *Handbook of Mathematical Functions*, Dover Publ., New York.
- Acton L. W., Feldman, U. *et al.*: 1992, *Publ. Astron. Soc. Japan* **44**, L71.
- Brown, J. C.: 1971, *Solar Phys.* **18**, 489.
- Brown, J. C.: 1975, in S. R. Kane (ed.), 'Solar Gamma-, X-, and EUV Radiation', *IAU Symp.* **68**, 245.
- Brown, J. C. and McClymont, A. N.: 1975, *Solar Phys.* **41**, 135.
- Dennis, B. R.: 1988, *Solar Phys.* **118**, 49.
- Doschek, G. A. *et al.*: 1990, in M. R. Kundu, B. Woodgate, and E. J. Schmahl (eds.), *Energetic Phenomena on the Sun*, Kluwer Academic Publishers, Dordrecht, Holland, p. 305.
- Feldman, U.: 1990, *Astrophys. J.* **364**, 322.
- Feldman, U., Hiei, E., Phillips, K. J. H., Brown, C. M., and Lang, J.: 1994, *Astrophys. J.* **421**, 843.
- Forbes, T. G. and Malherbe, J. M.: 1986, *Astrophys. J.* **302**, L67.
- Kosugi, T.: 1993, in J. F. Linsky and S. Serio (eds.), 'Physics of Solar and Stellar Coronae', *G. S. Vaiana Memorial Symposium*, Kluwer Academic Publishers, Dordrecht, Holland, p. 131.
- Leach, J. and Petrosian, V.: 1981, *Astrophys. J.* **251**, 781.
- Leach, J. and Petrosian, V.: 1983, *Astrophys. J.* **269**, 715.
- Lin, R. P., Schwartz, R. A., Pelling R. M., and Hurley, K. C.: 1981, *Astrophys. J.* **251**, L109.
- Masuda, S.: 1994, Ph.D. thesis, The Yohkoh HXT Group, National Astronomical Observatory, Mitaka, Tokyo 181, Japan.
- Masuda, S., Kosugi, T., Hara, M., Tsuneta, S., and Ogawara, Y.: 1994, *Nature* **371**, 371.

- Melrose, D. B. and Dulk, G. A.: 1984, *Astrophys. J.* **282**, 308.
- Melrose, D. B. and White, S. M.: 1981, *J. Geophys. Res.* **86**, 2183.
- Spitzer, L.: 1962, *Physics of Fully Ionised Gases*, Interscience, New York.
- Takakura, T., Inada, M., Makishima, K., Kosugi, T., Sakao, T., Masuda, S., Sakurai, T., and Ogawara, Y.: 1993, *Publ. Astron. Soc. Japan* **45**, 737.
- Tsuneta S., Acton, L., Bruner, M., Lemen, J., Brown, W., Carvalho, R., Catura, R., Freeland, S., Jurcevich, B., Morrison, M., Ogawara, Y., Hirayama, T., and Owens, J.: 1991, *Solar Phys.* **136**, 37.